I&EC research
Industrial & Engineering Chemistry Research

Article

Silica Nanoparticle Enhancement in the Efficiency of Surfactant Flooding of Heavy Oil in a Glass Micromodel

Goshtasp Cheraghian, Sajad Kiani, Nashaat N. Nassar, Shirin Alexander, and Andrew R Barron

Ind. Eng. Chem. Res., **Just Accepted Manuscript** • DOI: 10.1021/acs.iecr.7b01675 • Publication Date (Web): 11 Jul 2017

ACS Publications

Industrial & Engineering Chemistry Research is published by the American Chemical Society. 1155 Sixteenth Street N.W., Washington, DC 20036

Submitted to: *Ind. Eng. Chem. Res.*

Silica Nanoparticle Enhancement in the Efficiency of Surfactant Flooding of Heavy Oil in a Glass Micromodel

Goshtasp Cheraghian,[†] Sajad Kiani,[‡] Nashaat N. Nassar,[§] Shirin Alexander[#‡] and Andrew R. Barron[‡,#*]*

[†] Young Researchers and Elite Club, Omidieh Branch, Islamic Azad University, Omidieh, Iran

[§] Department of Chemical and Petroleum Engineering, University of Calgary, 2500 University Drive NW, Calgary, Alberta, Canada

[‡] Energy Safety Research Institute (ESRI), Swansea University, Bay Campus, Swansea SA1 8EN, UK

[#] Department of Chemistry and Department of Materials Science and Nanoengineering, Rice University, Houston, Texas 77005, USA

ABSTRACT: The synergic effects of fumed-Si nanoparticles (Si-NPs) in combination with sodium dodecyl sulfate (SDS) surfactant as suitable agents for oil displacing in enhanced oil recovery (EOR) are evaluated using a 5-spot glass micromodel. Optimum oil recovery (45%) is obtained for SDS near the critical micelle concentration; however, the addition of fumed silica nanoparticles (Si-NPs) enables a further 13% enhancement in oil recovery for the maximum concentration of the SDS/Si-NPs (2.2 wt.%), as well as delaying the breakthrough point. The optimum mass ratio of SDS:Si-NP (1:11) suggests that the Si-NPs are aggregated by the SDS micelles; consistent with increased viscosity upon addition of Si-NPs. The presence of the Si-NPs also greatly increases the wettability on the glass surface, with a decrease in the contact angle from 73° for SDS (1800 ppm) to 11° for SDS/Si-NPs (1800 ppm/2.0 wt.%). The effective changes in the oil sweeping mechanism are directly observed in glass micromodel and correlate to these physical measurements. The results demonstrated the addition of Si-NPs to SDS solutions made a significant improvement to oil recovery values and potentially beneficial in EOR applications.

KEYWORDS: Fumed-silica nanoparticles; micro-model test; enhanced oil recovery; Sodium dodecyl sulfate

Submitted to: *Ind. Eng. Chem. Res.*

1. INTRODUCTION

As oil fields mature the need to maximize production of existing capacity as opposed to develop new production becomes vital to meet the worlds increasing energy demands. Enhanced oil recovery (EOR), also known as tertiary recovery, is the application of different physical and chemical methods for increasing crude oil extraction. The injection of water has been used to aid mobility, which in combination with chemical additives allows for the reduction in the interfacial tension (capillary pressure) that hampers oil droplets from moving through a reservoir. This oil sweeping technique has shown an enormous potential through the use of novel surfactants, polymers, and nanomaterials.[1,2]

Laboratory glass micromodel experiments have been applied to the study of particle movement, microgeometry, and physical characteristics of liquids, gases, and solids through porous media.[3-5] Such micromodel experiments have been used to investigate the mechanism of the fluid flow on porous mediums via flow visualization, fluid interactions, pore space geometry, topology and heterogeneity effects, which are not possible to assess using traditional coreflood experiments. Recently, micromodels with various etched visible flow patterns have been utilized to cover the foam blocking mechanism and oil mobility control.[6,7] However, the viral pore shape pattern in the micromodel is triangular in structure, which has more similarity to the actual reservoir conditions of the NPs distribution in porous media.[8]

Recent studies on etched-glass micromodels have shown insight into EOR mechanisms and oil displacing processes involving immiscible fluids.[4,9] Wu et al.[5] evaluated the pore-scale mobility, residual oil saturation and the rate of oil sweeping in the foam flooding with heavy oil. Mohammadi et al.[3] demonstrated how to record the variation of oil sweeping in micromodels and they studied the influence of reservoir heterogeneity as an important parameter on oil recovery with a two-dimensional micromodel. The various common flooding methods that are often used in EOR (water, gas, WAG and surfactant flooding) for enhancing the sweep efficiency and oil displacement have been investigated.[10] Surfactant flooding studies using this model have displayed promising results for recovering trapped and residual oil.[11] One of the important approaches to maximize oil sweeping is using an appropriate surfactant, which results in fluid viscosity alteration and the IFTs between rock-fluid and fluid-fluid.[12] Key experiments have revealed that the presence of NPs and surfactants have a high potential to decrease the strong interactions taking place between

interfaces in porous mediums,[13-18] while various nanomaterials such as clay, SiO_2, MgO, TiO_2, ZrO, NiO and Al_2O_3 have been employed using light to extra heavy oil in various EOR methods.[19-24]

It has been reported that the use of fumed-Si nanoparticles (Si-NPs) in water flooding would increase the oil production from hydrocarbon reservoirs to around 50-75% in secondary and tertiary oil recovery.[25] In this context, we report herein, the first use of Si-NPs in combination with SDS solutions for flood experiments in a five-spot micromodel. The behavior of NPs at various SDS concentrations was evaluated. The results of this paper are directed as a new approach and sheds light on the value of using Si-NPs in EOR applications.

2. EXPERIMENTAL SECTION

2.1. Materials. Fumed-silica (Aerosil 300), and sodium dodecyl sulfate ($C_{12}H_{24}SO_4Na$, M_W = 288.38) were purchased from Degussa Chemicals (Hanau, Germany), Central Drug House (P) Ltd. The fumed-silica nanoparticles (Si-NPs) had a measured mean particle diameter of 20-80 nm (Figure S1, see SI), with a specific surface area, pH, and SiO_2 purity of 300 $m^2.g^{-1}$, 3.7-4.7, and 99.8 wt.%, respectively. Sodium chloride (NaCl), sodium sulfite (Na_2SO_3), calcium chloride ($CaCl_2$), magnesium chloride hexahydrate ($MgCl_2.6H_2O$), and sodium bicarbonate (Na_2HCO_3), and ethanol (C_2H_5OH) were used as received from Sigma-Aldrich. The oil sample (dead oil) was supplied from a heavy oilfields located in the South of Iran (API: 17° @ 25 °C) The density and viscosity of crude oil were measured as 973 $kg.m^{-3}$ and 1320 mPa.s, respectively. Distilled water was used throughout the experiments. A synthetic sea brine sample was used for experiment tests, with total dissolved solids (TDS) of 2 wt.% was as a mixture of NaCl (1.71 wt.%), Na_2SO_3 (0.01 wt.%), $CaCl_2$ (0.32 wt.%), $MgCl_2.6H_2O$ (0.09 wt.%) and Na_2HCO_3 (0.02 wt.%).

2.2. Characterization. The sample weight loss measurement determined by thermogravimetric/differential thermal analysis (TG/DTA) and was performed using a TGA/SDT A851 Mettler Toledo instrument. The samples were run in an open alumina crucible under continuous air flow. The heating profile was equilibrated at 50 °C and then ramped at 10 $°C.min^{-1}$. Transmission electron microscopy (TEM) was carried out using a Phillips EM 208 to determine the size, and morphology of the nanoparticles. The viscosities of the samples were measured with Brookfield viscometer model DV-III Ultra (Brookfield Instruments) with a small scale sample adapter and spindle no. 21 at 25 °C. A thermostat

Submitted to: *Ind. Eng. Chem. Res.*

water bath was used to maintain the temperature of the sample through a water jacket fitted to the small sample adapter. The bath temperature was maintained with an accuracy of 1 °C. The viscosity measurements were repeated three times each and the averages of the readings were taken for the data analysis. Sessile Drop (Kruss G10, Germany) was used to measure the static contact angles of crude oil, SDS and SDS/Si-NPs solutions on a microscope glass at room temperature. The data are an average of five measurements taken from various positions on the surface. Nikon LV100D optic microscope was used for the pore-throat and solution pathways images. The electrical conductivity measurements were performed using a Crison conductivity meter (Basic 30). The conductometer probe was washed with distilled water and calibrated using standard solution after each measurement. Different concentrations of SDS solutions were made in water and their conductivities were measured at ambient condition.

2.3. Micromodel Experimental. The micromodel was composed of two glass plates and two drilled ports (inlet and outlet; 3 mm). The etched plate and the cover plate are brought together and sealed by implementing a special technique to form an enclosed pore space. This technique can be used for various types of reservoir conditions (water, oil, and gas), and has a pattern area of 6.5×6.5 cm^2 etched flow network.[20] The properties of the resulting micromodel are shown in Table 1.

Table 1. Properties of the glass micromodel.

Pore diameter (μm)	Throat diameter (μm)	Permeability (mD)	Porosity (%)	Etched thickness (μm)
650	280	4.5	33	45

The schematic of the micromodel pattern is shown in Figure 1. The design of the micromodel is simple and contains a fluid injection section (a syringe pump), an optical system that exposures light on fluid pattern, and a micro-model holder. Various solutions with different pore volumes were prepared to run each test in a glass micromodel using a Quizix pump. At the beginning of each run, the micromodel was saturated with brine until the system became free of air and bubbles (i.e., water saturation). Oil constantly injected through the channels and system was fully saturated with oil (100% initial oil saturation). Then, the micromodel was aged in oil for two weeks (to be strongly oil-wet). Finally, SDS and SDS/Si-

NPs solutions were injected using a pump at the constant injection flow rate (0.0006 cm^3/min) and residual oil saturation to assess the amount of oil remaining was carried out after each flooding test by differences between initial original oil saturation and residual oil saturation values using image processing. Finally, SDS and SDS/Si-NPs solutions were injected at a constant injection flow rate (0.0006 cm^3/min). After each flooding, residual oil saturation to assess the amount of oil remaining was carried out. The residual oil saturation analyses in pores and pore-throats were studied using image processing. The micromodel was cleaned between each individual run: The relevant cleaning fluids (distilled water, methylene chloride, acetone, and toluene) were applied using a syringe pump. The micromodel was dried in an oven at 70 °C for 2 h. Pressure monitoring was measured by the high-sensitive resolution of transducer and high-accuracy low-flow-rate Quizix pump was used to control the injection fluids through the glass micromodel.[8]

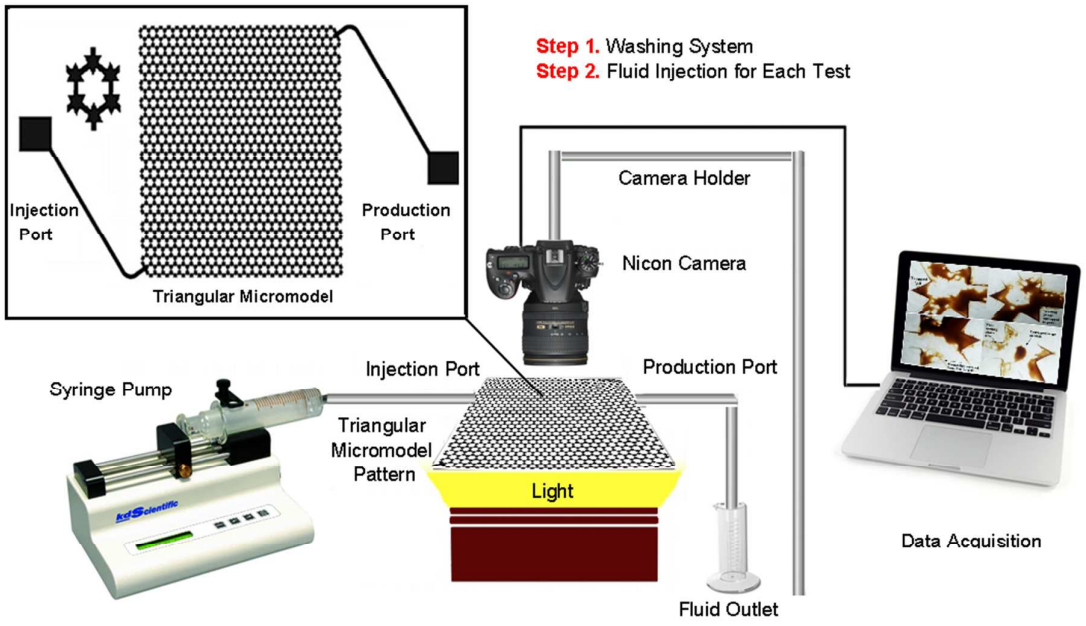

Figure 1. Schematic of micromodel experimental set-up.

3. RESULTS AND DISCUSSION

Prior to investigation of the synergic effects between the fumed-Si nanoparticles (Si-NPs) and the sodium dodecyl sulfate (SDS) surfactant, we determined the concentration effects of SDS concentration alone. The critical micelle concentration (CMC) of SDS solution was determined by measuring the break point in the conductivity plot (Figure S2, see SI).[26,27, 28]

Submitted to: *Ind. Eng. Chem. Res.*

Based on these results the CMC value of SDS is 1824 ppm under the conditions employed in the micromodel system (see Experimental). Thus, surfactant micromodel injection experiments were carried out at different SDS concentrations around the optimum CMC value, i.e., 1600, 1800 and 2000 ppm.

The oil recovery (%) was measured using the micromodel system (see Experimental). Representative oil recovery values as a function of pore volume injected (PVI) for SDS solutions are shown in Figure 2. Due to the symmetry of pores in the micromodel, the path the injected liquid choses to follow when displacing the fluid inside the porous media is essentially constant for similar compositions making comparison between compositional data meaningful. As can be seen from Figure 2, the oil recover increases with SDS concentration between 1600 and 1800 ppm; however, no further increase is observed at greater concentrations. It is interesting to note that at the beginning of the experiments when SDS solution was injected (PVI = 1), the oil recovery increases by increasing the SDS concentration. However, at higher pore volumes (where a great amount of injected fluid is being produced) the oil recovery is not affected by the SDS concentration (2.1 - 2.2 PVI). As a result, and considering the cost of surfactants and the environmental issues of using chemicals, the smallest concentration at which the best results are obtained (1800 ppm SDS) was chosen for the follow-up experiments.

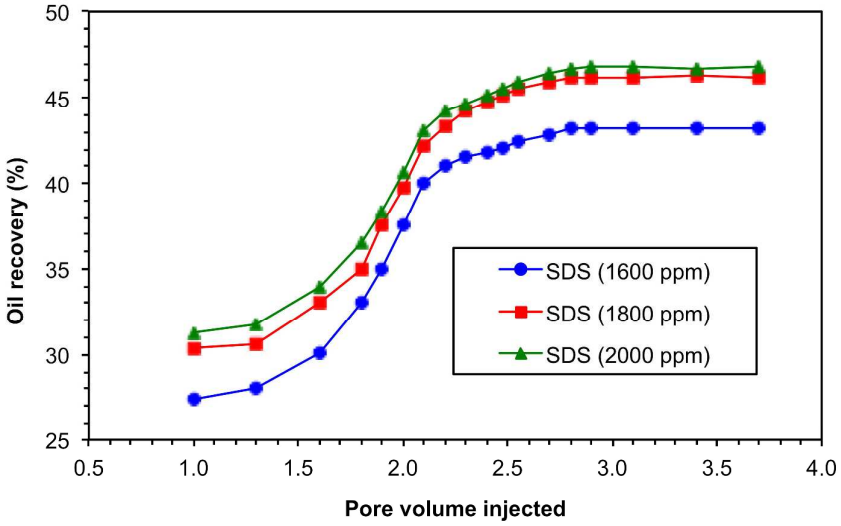

Figure 2. Oil recovery (%) obtained using the micromodel set up using various SDS concentrations.

Submitted to: *Ind. Eng. Chem. Res.*

The effect of SDS/Si-NPs solutions on oil recovery was examined by adding three different Si-NPs concentrations to a constant concentration SDS solution (1800 ppm): 1.8, 2.0 and 2.2 wt%. As can be seen in Figure 3, the addition of 1.8 wt% Si-NP to 1800 ppm SDS results in a similar recovery as SDS alone until a PVI of 2.3, above which there is a divergence with a concomitant shift in the breakthrough point (from 2.1-2.2 PVI for SDS to 2.55-2.7 for SDS/Si-NP). The increase in oil recovery is further enhanced by an increase in the Si-NP content up to 2 wt%, above which no further enhancement is observed. The breakthrough appears to be unaffected by the Si-NP content. The results indicate an increase of up to 13% oil recovery for the maximum concentration of the SDS/Si-NPs (2.2 wt.%), compared to the SDS solutions alone. Cheraghian et al. has reported that titanium dioxide NPs improved oil recovery in the peresence of surfactans at around their CMC values.[29]

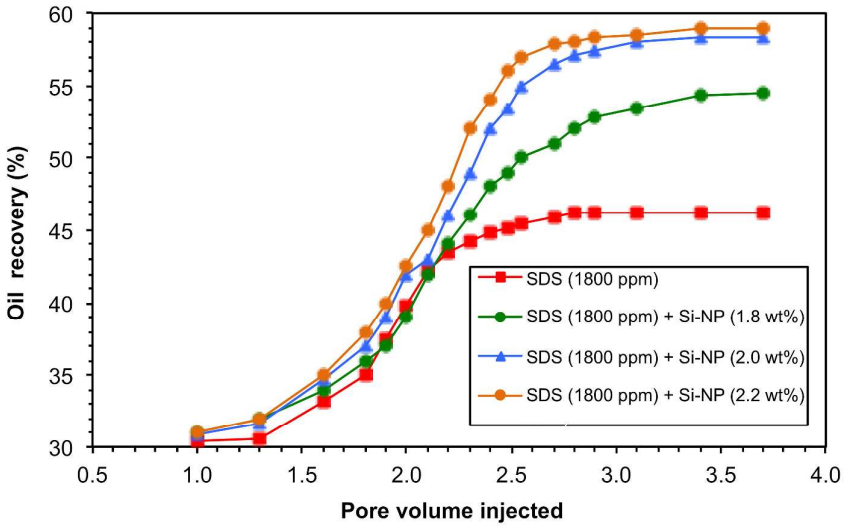

Figure 3. Plot of oil recovery (%) as measured using the micromodel system, as a function of the pore volume injected, for various concentrations of Si-NPs (1.8, 2.0, and 2.2 wt.%) added to 1800 ppm SDS.

A qualitative illustration of SDS and SDS/Si-NPs solutions injection at different stages are shown in Figure 4 and 5, respectively. Figure 4 shows the fluid distribution in the micromodel during SDS (1800 ppm) injection. The black areas are the micromodel pathways, which are saturated with oil before SDS injection. Based on the image, as the SDS solution comes in contact with oil and as time passes during the injection, the channeling caused by the surfactant solution increases toward the outlet (Figure 4c) due to relatively low viscosity of the displacing fluid (SDS solution). In contrast, the SDS/Si-NPs solution form more

Submitted to: *Ind. Eng. Chem. Res.*

uniform sweeping during the injection and larger oil areas are covered by the solution, as is illustrated in Figure 5. As shown in Figure 4 and 5, the frontal structure through the micromodel is affected by the choice of SDS versus SDS/Si-NPs. We propose that SDS flooding results in viscous fingering due to the low viscosity of SDS in water compared to the oil, whereas the results for SDS/fumed-SiNPs is owing to homogenous front in micromodel. Therefore, the decrease in the channeling during SDS/fumed-SiNPs injection (because of increase in viscosity of the displacing fluid and possibly adsorption of fumed-SiNPs at interfaces[30]) results in improved oil sweeping towards the outlet of the micromodel, and therefore higher percentages of oil recovery.

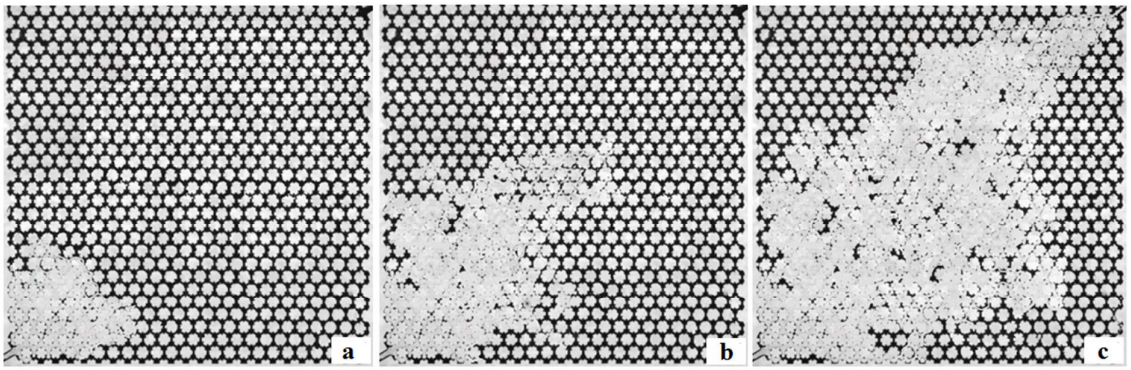

Figure 4. Qualitative illustration effect of SDS injection (1800 ppm) in the micromodel setup, at three sequential displacement time stages of (a) 180s, (b) 480s, and (c) 1020s.

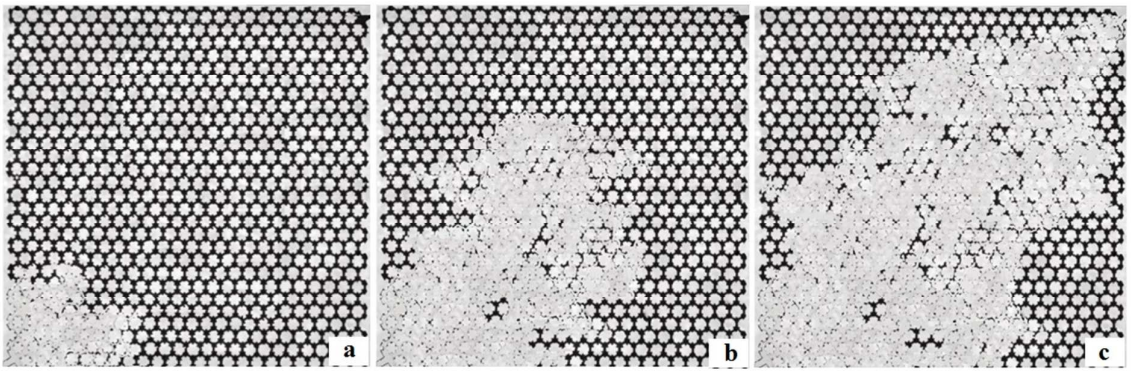

Figure 5. Qualitative illustration effect of SDS/SiNPs injection (2.0 wt.%) at three sequential displacement time stages of (a) 180s, (b) 480s, and (c) 1020s.

Submitted to: *Ind. Eng. Chem. Res.*

Microscopic images of SDS and SDS/Si-NPs flooding through the pores of the glass micromodel are shown in Figure 6. Figure 6a shows the fluid distribution of SDS injection, which certainly affects the trapped oil and the amount of oil saturation after the surfactant flooding. Figure 6b shows the oil spreading through the micromodel pores in the presence of SDS solution. This condition shows the glass micromodel shifts toward water-wet than oil-wet medium. The majority of oil had remained in the corner of the pores after flooding which comes from the strong adhesion forces, which avoids oil displacing through the pores with SDS flooding. As is shown in Figures 6c and d, SDS/Si-NPs flooding results in the improvement in oil sweeping especially changes towards a strong water-wet medium compared to SDS flooding alone. The visualization results have shown that the amount of residual oil saturation through the pores and pore-throats after SDS/fumed SiNPS flooding is lower than SDS flooding. These results suggest that change in surfactant adsorption and wettability (due to bonding interactions between surfactant and NPs)[31] are possible mechanisms for 13% improvement in oil recovery in the presence of SDS/Si-NPs (over SDS alone).

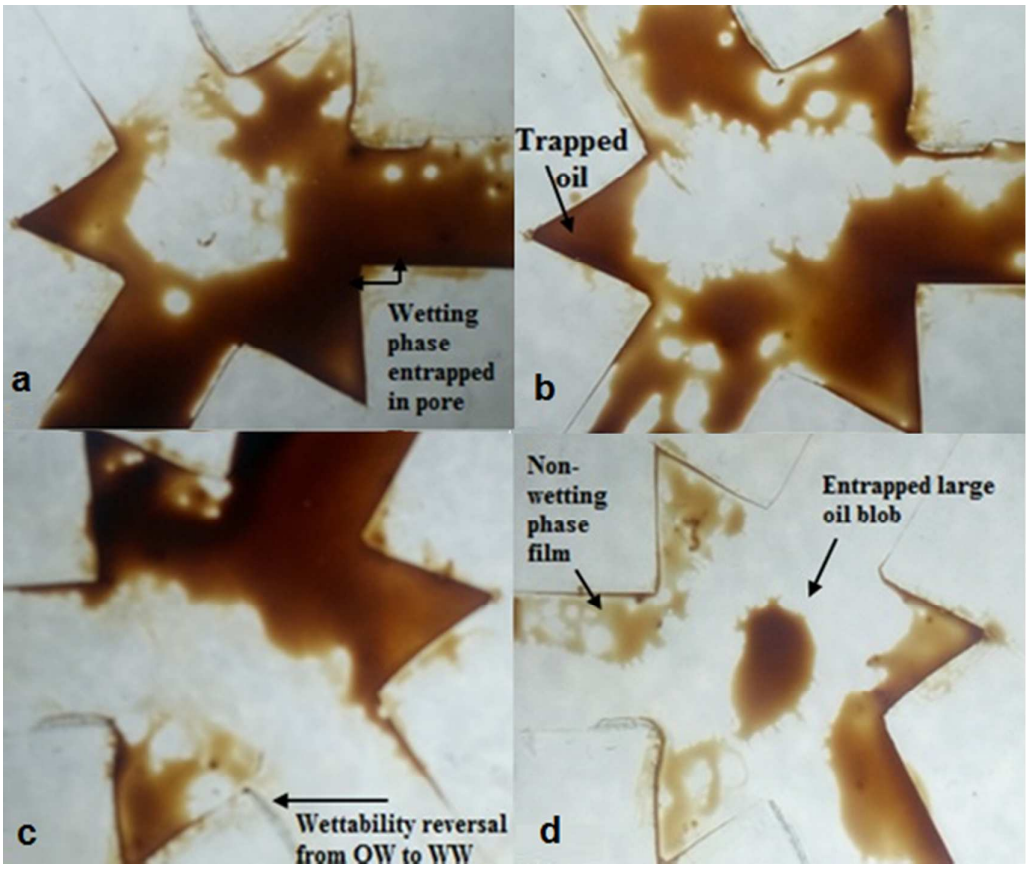

Submitted to: *Ind. Eng. Chem. Res.*

Figure 6. Digital microscope images of solution injection in the micromodel showing the pore-scale configuration and distribution of wetting and non-wetting phases within an initially preferential oil-wet medium for (a and b) SDS (1800 ppm) and (c and d) SDS/Si-NPs (1800 ppm/2 wt.%).

Clearly the addition of Si-NPs to SDS results in a significant enhancement on oil recovery (Figure 3) as well as enhanced pore clearing (Figure 6); however, the chemical interactions are of interest. The thermogravimetric/differential thermal analysis (TG/DTA) of the dried samples for SDS (1800 ppm) and SDS/Si-NPs (1800 ppm/2.0 wt.%) were carried out under air (Figure S3, see SI). The major affect of adding Si-NPs appear to be a shift to higher temperatures (350 °C) of the major exotherm observed for SDS decomposition (280 °C), consistent with bonding of surfactant on the surface of Si-NPs.[32,33]

As noted above, Figures 6 appears to suggest that the enhancement in oil recovery could be due to a change in wettability. In order to evaluate the effect of SDS and SDS/Si-NPs on wettability, contact angle measurements were carried out (Table 2). The influence of fluid-solid interaction on contact angle measurements in glass micromodel systems has been investigated in previous literatures.[34-36] Figures 7a and b shows the contact angles of crude oil and SDS solutions at around 102º and 73º, respectively. In contrast, the contact angle of SDS/Si-NPs decreased to 11º (Figure 7c). The presence of NPs significantly changes the strong physiochemical interactions taking place between fluid-solid interfaces and can result in positive wettability alteration for oil extraction.[37,38]

Table 2. Contact angles (º) of liquid-solid interface of different solutions.

Materials	Contact angle (º)
Crude oil	102.2 ±0.8
SDS (1600 ppm)	76±1
SDS (1800 ppm)	72.5±0.5
SDS (2000 ppm)	68.8±0.2
SDS/Si-NPs (1600 ppm/1.8 wt.%)	13.0±0.5
SDS/Si-NPs (1800 ppm/2.0 wt.%)	11±1
SDS/Si-NPs (2000 ppm/2.2 wt.%)	9.8±0.5

Submitted to: *Ind. Eng. Chem. Res.*

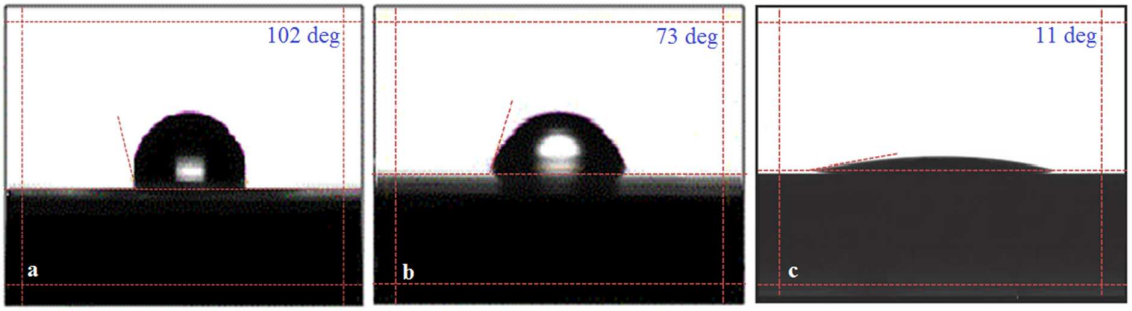

Figure 7. Contact angle measurement (a) crude oil, (b) SDS (1800 ppm), and (c) SDS/Si-NPs (1800 ppm/2.0 wt.%).

Effective oil sweeping through porous media toward the production wells depends greatly on optimum fluid viscosity. Rheological measurements for SDS and SDS/Si-NPs solutions were characterized with a rotational viscometer at room temperature. Figure 8 shows the effect of shear rate on viscosity for the SDS (1800 ppm) and SDS/Si-NPs (1800 ppm/2.0 wt.%) samples. At a lower shear rate value (100 s^{-1}) the viscosity of SDS/Si-NPs was significantly higher compared to the SDS solutions alone. Both samples fit the Power Law (or Ostwald) model (Eq. 1), where: η is the viscosity, $\dot{\gamma}$ is the shear rate, K is the consistency (viscosity at a shear of 1 s^{-1}) and *n* is the Power law index. As may be seen from Table 3 both samples behave as shear-thinning (pseudo-plastic) fluids; consistent with the observed non-linear relationship between shear rate and shear stress (Figure S2). However, SDS (1800 ppm) is closer to Newtonian that SDS/Si-NPs (1800 ppm/2.0 wt.%). Given that the mass ratio of SDS/Si-NPs in the 1800 ppm/2.0 wt.% sample is ca. 1:11 and that the typical SDS micelle is 2 nm in diameter as compared 20-80 nm for the Si-NPs, it unreasonable to propose that the SDS forms monolayer coverage of the Si-NPs. Instead it is more likely that the Si-NPs are aggregated by the micelles, forming large aggregates relatively stable aggregates.[39]

$$\eta = K\dot{\gamma}^{\,n-1} \qquad (1)$$

Table 3. Power law (Ostwald) parameters.

Materials	Consistency (mPa.s)	Power law (flow) index
SDS (1800 ppm)	4.9	0.82

Submitted to: *Ind. Eng. Chem. Res.*

SDS/Si-NPs (1800 ppm/2.0 wt.%)	565	0.25

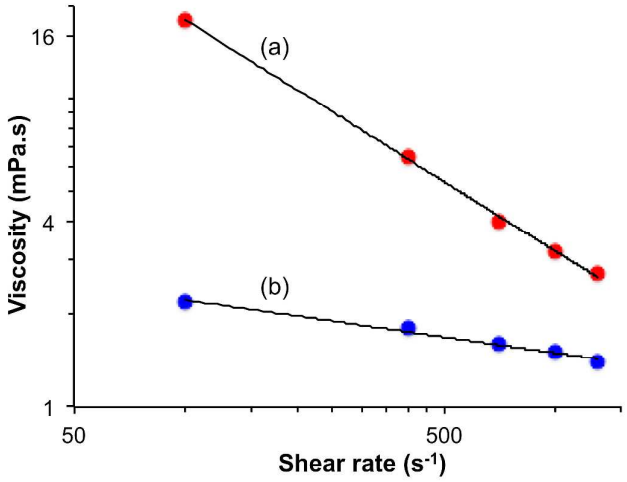

Figure 8. Plot of viscosity (mPa.s) as a function of shear rate (s^{-1}) for (a) SDS (1800 ppm) and (b) SDS/Si-NPs (1800 ppm/2.0 wt.%), R^2 = 0.998 and 0.989, respectively.

Additional insight into the mechanistic differences between SDS and SDS/Si-NP solutions is obtained by visual inspection of the cross section of the micro channels. Figure 9 shows schematic representations (a and b) with representative photographic images (c and d). As shown in Figure 9a and c, the first mechanism is related to the effect of SDS injection through oil pathway. In this case, there are sufficient oil recoveries, stemming from the SDS injection through the glass micromodel. However, the relatively low viscosity of surfactant solutions compared to oil, leads to channel formation and maximum oil recovery is ~45%. Upon addition of Si-NPs, oil displacement has changed through the micromodel pathway, which is shown in Figure 8b and d, due to an increase in the viscosity of the solution and results in displacement the larger amount of oil toward the micromodel outlet (up to ~ 58%).

Submitted to: *Ind. Eng. Chem. Res.*

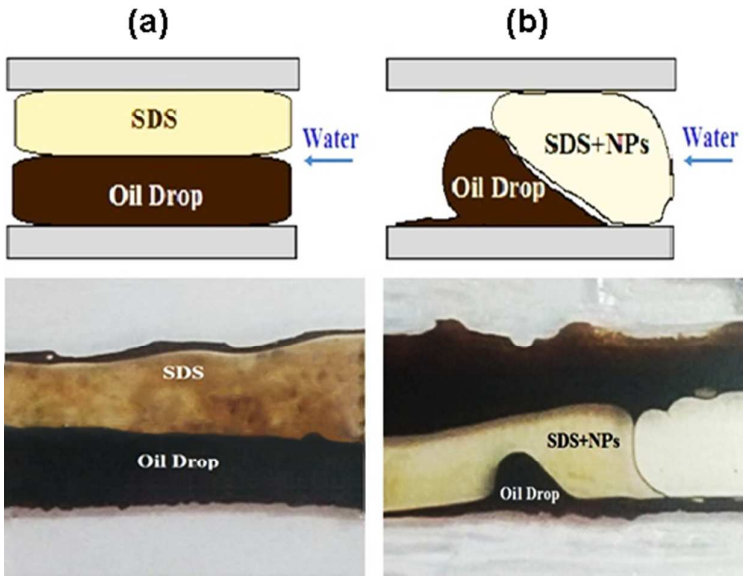

Figure 9. Displacement differences on five-spot micromodel (a) SDS injection (1800 ppm), and (b) SDS/Si-NPs injection (1800 ppm/2.0 wt%).

4. CONCLUSIONS

The effect of Si-NPs on surfactant (SDS) mediated oil recovery has been investigated using a 5-spot triangular glass micromodel as a porous medium. The effect of Si-NPs on wettability and viscosity were also determined. The result indicated that the presence of Si-NPs significantly improved the heavy oil recovery in the micromodel test, possibly due to the improvement in SDS adsorption, in the presence of NPs during the surfactant injection.The addition of Si-NPs to the surfactant solution leads to flow modification due to a change in viscosity. The viscosity values of the SDS/NPs solution were more than double the values of the surfactant solution alone. The contact angle data indicated that SDS/Si-NPs injection altered the wettability from oil wet to water-wet condition as a result of the hydrophilic nature of SiO_2 nanoparticles. Consequently, SDS/Si-NPs solution can be used as an additive towards effective wettability alteration in oil reservoirs. Laboratory results showed that ultimate oil recovery by injection of 2 wt.% SiNPs in SDS was 13% higher than the ultimate oil recovery by surfactant alone. The results of this work support an improved insight into the role of Si-NPs and surfactants in enhanced oil recovery and future use in EOR formulations. We note that is some oil field applications the cost of NPs is prohibitive;[40] however, in the present case we suggest that the increased performance and change in sweep mechanism could possibly outweigh upfront cost issues.

Submitted to: *Ind. Eng. Chem. Res.*

AUTHOR INFORMATION

Corresponding Authors

*E-mail: goshtasbc@gmail.com (GC) and a.r.barron@swansea.ac.uk (A.R.B.)

Notes

The authors declare no competing financial interest.

ACKNOWLEDGMENT

Financial support was provided by the Sêr Cymru II Welsh Fellowship part-funded by the European Regional Development Fund (ERDF) (S.A.), the Welsh Government Sêr Cymru Programme, through the Sêr Cymru Chair for Low Carbon Energy and Environment, FLEXIS, which is part-funded by the European Regional Development Fund (ERDF) through the Welsh Government, and the Robert A. Welch Foundation (C-0002) (A.R.B.), and Research Branch of the Islamic Azad University, Iran (G.C). We thank Prof. Ole Torsaeter at University of NTNU for advices.

SUPPORTING INFORMATION

Rheological properties of SDS and SDS/SiNPs under different shear stress. Phase studies of oil/SDS/Si-NPs. SEM, XRD, and TG/DTA.

REFERENCES

(1) Pei, H.; Zhang, G.; Ge, J.; Tang, M.; Zheng, Y. Comparative effectiveness of alkaline flooding and alkaline–surfactant flooding for improved heavy-oil recovery. *Energy Fuels* **2012**, *26*, 2911-2919.

(2) Wei, B.; Li, Q.; Jin, F.; Li, H.; Wang, C. The potential of a novel nanofluid in enhancing oil recovery. *Energy Fuels* **2016,** *30*, 2882-2891.

(3) Mohammadi, S.; Ghazanfari, M. H.; Masihi, M. A pore-level screening study on miscible/immiscible displacements in heterogeneous models. *J. Pet. Sci. Eng.* **2013**, *110*, 40-54.

(4) Jeong, S.-W.; Corapcioglu, M. Y.; Roosevelt, S. E. Micromodel study of surfactant foam remediation of residual trichloroethylene. *Environ. Sci. Technol.* **2000**, *34*, 3456-3461.

(5) Wu, Z.; Liu, H.; Pang, Z.; Wu, C.; Gao, M. Pore-scale experiment on blocking characteristics and eor mechanisms of nitrogen foam for heavy oil: a 2D visualized study. *Energy Fuels* **2016**, *30*, 9106-9113.

(6) Li, R. F.; Yan, W.; Liu, S.; Hirasaki, G.; Miller, C. A. Foam mobility control for surfactant enhanced oil recovery. *SPE J.* **2010**, *15*, 928-942.

(7) Gauteplass, J.; Chaudhary, K.; Kovscek, A. R.; Fernø, M. A. Pore-level foam generation and flow for mobility control in fractured systems. *Colloids Surf., A* **2015**, *468*, 184-192.

(8) Meybodi, H. E.; Kharrat, R.; Araghi, M. N. Experimental studying of pore morphology and wettability effects on microscopic and macroscopic displacement efficiency of polymer flooding. *J. Pet. Sci. Eng.* **2011**, *78*, 347-363.

(9) Kim, Y.; Wan, J.; Kneafsey, T. J.; Tokunaga, T. K. Dewetting of silica surfaces upon reactions with supercritical CO_2 and brine: pore-scale studies in micromodels. *Environ. Sci. Technol.* **2012**, *46*, 4228-4235.

(10) Conn, C. A.; Ma, K.; Hirasaki, G. J.; Biswal, S. L. Visualizing oil displacement with foam in a microfluidic device with permeability contrast. *Lab Chip.* **2014**, *14*, 3968-3977.

(11) Jamaloei, B. Y. Insight into the chemistry of surfactant-based enhanced oil recovery processes. *Recent Pat. Chem. Eng.* **2009**, *2*, 1-10.

(12) Almalik, M. S.; Attia, A. M.; Jang, L. K. Effects of alkaline flooding on the recovery of Safaniya crude oil of Saudi Arabia. *J. Pet. Sci. Eng.* **1997**, *17*, 367-372.

(13) Amanullah, M.; Al-Tahini, A. M. In *Nano-technology-its significance in smart fluid development for oil and gas field application*, SPE Saudi Arabia Section Technical Symposium, 2009; Society of Petroleum Engineers: 2009.

(14) Xu, K.; Zhu, P.; Colon, T.; Huh, C.; Balhoff, M. A Microfluidic investigation of the synergistic effect of nanoparticles and surfactants in macro-emulsion-based enhanced oil recovery. *SPE J.* **2017**, *22*, 179691.

(15) Hashemi, R.; Nassar, N. N.; Pereira Almao, P. Enhanced heavy oil recovery by in situ prepared ultradispersed multimetallic nanoparticles: A study of hot fluid flooding for Athabasca bitumen recovery. *Energy Fuels* **2013**, *27*, 2194-2201.

(16) Sun, Q.; Li, Z.; Li, S.; Jiang, L.; Wang, J.; Wang, P. Utilization of surfactant-stabilized foam for enhanced oil recovery by adding nanoparticles. *Energy Fuels* **2014**, *28*, 2384-2394.

(17) Nguyen, P.; Fadaei, H.; Sinton, D. Pore-scale assessment of nanoparticle-stabilized CO_2 foam for enhanced oil recovery. *Energy Fuels* **2014**, *28*, 6221-6227.

(18) Zhang, H.; Nikolov, A.; Wasan, D. Enhanced oil recovery (EOR) using nanoparticle dispersions: underlying mechanism and imbibition experiments. *Energy Fuels* **2014**, *28*, 3002-3009.

(19) Yu, H.; He, Y.; Li, P.; Li, S.; Zhang, T.; Rodriguez-Pin, E.; Du, S.; Wang, C.; Cheng, S.; Bielawski, C. W. Flow enhancement of water-based nanoparticle dispersion through microscale sedimentary rocks. *Sci. Rep.* **2015**, *5*, 8702.

(20) Cheraghian, G. An experimental study of surfactant polymer for enhanced heavy oil recovery using a glass micromodel by adding nanoclay. *Pet. Sci. Technol.* **2015**, *33*, 1410-1417.

(21) Cheraghian, G.; Khalilinezhad, S. Effect of nanoclay on heavy oil recovery during polymer flooding. *Pet. Sci. Technol.* **2015**, *33*, 999-1007.

(22) Cheraghian, G. Application of nano-fumed silica in heavy oil recovery. *Pet. Sci. Technol.* **2016**, *34*, 12-18.

(23) Cheraghian, G.; Khalili Nezhad, S. S.; Bazgir, S. Improvement of thermal stability of polyacryl amide solution used as a nano-fluid in enhanced oil recovery process by nanoclay. *Int. J. Nanosci. Nanotech.* **2015**, *11*, 201-208.

(24) Kiani, S.; Samimi, A.; Rashidi, A. Novel one-pot dry method for large-scale production of nano γ-Al2. *Monatsh. Chem.* **2016**, *147*, 1153-1159.

(25) Green, D. W.; Willhite, G. P. Enhanced oil recovery. Henry L. Doherty Memorial Fund of AIME. *Society of Petroleum Engineers: Richardson, TX* **1998**.

(26) Ahmadi, M. A.; Shadizadeh, S. R. Adsorption of novel nonionic surfactant and particles mixture in carbonates: enhanced oil recovery implication. *Energy Fuels* **2012**, *26*, 4655-4663.

(27) Azam, M. R.; Tan, I. M.; Ismail, L.; Mushtaq, M.; Nadeem, M.; Sagir, M. Static adsorption of anionic surfactant onto crushed Berea sandstone. *J. Pet. Explor. Prod. Technol.* **2013**, *3*, 195-201.

(28) Kiani, S.; Mansouri Zadeh, M.; Khodabakhshi, S.; Rashidi, A.; Moghadasi, J. Newly prepared Nano gamma alumina and its application in enhanced oil recovery: an approach to low-salinity waterflooding. *Energy Fuels* **2016**, *30*, 3791-3797.

(29) Cheraghian, G. Effects of titanium dioxide nanoparticles on the efficiency of surfactant flooding of heavy oil in a glass micromodel. *Pet. Sci. Technol.* **2016**, *34*, 260-267.

(30) Li, R.; Jiang, P.; Gao, C.; Huang, F.; Xu, R.; Chen, X. Experimental investigation of silica-based nanofluid enhanced oil recovery: the effect of wettability alteration. *Energy Fuels* **2017**, 31, 188-197.

(31) Cheraghian, G.; Evaluation of clay and fumed silica nanoparticles on adsorption of surfactant polymer during enhanced oil recovery. *J. Jpn. Petrol. Inst.* **2017**, *60*, 85-94.

(32) Whitsitt, E. A.; Barron, A. R. Effect of surfactant on particle morphology for liquid phase deposition of submicron silica. *J. Colloid Interface Sci.* **2005**, *287*, 318-325.

(33) Lv, Q.; Li, Z.; Li, B.; Li, S.; Sun, Q. Study of nanoparticle–surfactant-stabilized foam as a fracturing fluid. *Ind. Eng. Chem. Res.* **2015**, *54*, 9468-9477.

(34) Wan, J.; Wilson, J. L. Visualization of the role of the gas-water interface on the fate and transport of colloids in porous media. *Water Resour. Res.* **1994**, *30*, 11-23.

(35) Grate, J. W.; Dehoff, K. J.; Warner, M. G.; Pittman, J. W.; Wietsma, T. W.; Zhang, C.; Oostrom, M. Correlation of oil–water and air–water contact angles of diverse silanized surfaces and relationship to fluid interfacial tensions. *Langmuir* **2012**, *28*, 7182-7188.

(36) Buckley, J. S.; Bousseau, C.; Liu, Y. Wetting alteration by brine and crude oil: from contact angles to cores. *SPE J.* **1996**, *1*, 341-350.

(37) Nazari Moghaddam, R.; Bahramian, A.; Fakhroueian, Z.; Karimi, A.; Arya, S. Comparative study of using nanoparticles for enhanced oil recovery: wettability alteration of carbonate rocks. *Energy Fuels* **2015**, *29*, 2111-2119.

(38) Giraldo, J.; Benjumea, P.; Lopera, S.; Cortés, F. B.; Ruiz, M. A. Wettability alteration of sandstone cores by alumina-based nanofluids. *Energy Fuels* **2013**, *27*, 3659-3665.

(39) Kumar, S.; Aswal, V. K.; Kohlbrecher, J. Size-dependent interaction of silica nanoparticles with different surfactants in aqueous solution. *Langmuir.* **2012**, *28*, 9288-9297.

(40) Morrow, L.; Potter, D.; Barron, A. R. Detection of magnetic nanoparticles against proppant and shale reservoir rocks. *J. Exp. Nanosci.* **2014**, *9*, DOI:10.1080/17458080.2014.951412

Submitted to: *Ind. Eng. Chem. Res.*

Graphical Abstract